ACOUSTIC SURFACE WAVE DEVICES FOR VISIBLE AND INFRARED IMAGING

Robert L. Gunshor

Purdue University

Prepared for:

Defense Advanced Research Projects Agency

1 January 1975

Semi-Annual Technical Report
for the Period 6/1/74 - 11/30/74

Acoustic Surface Wave Devices for Visible and Infrared Imaging

Grant Number DAHC15-73-G12

Program Code No. 4D10

Grantee: Purdue Research Foundation

Principle Investigator: R. L. Gunshor (317) 493-9488

Effective Date of Grant: 6/1/74

Grant Expiration Date: 5/31/75

Amount of Grant: $99,910

Sponsored by
Advanced Research Projects Agency
ARPA Order No. 2340 Amendment No. 1

UNCLASSIFIED

Security Classification

DOCUMENT CONTROL DATA - R&D

(Security classification of title, body of abstract and indexing annotation must be entered when the overall report is classified)

1. ORIGINATING ACTIVITY (Corporate author)

Purdue Research Foundation - School of Electrical Engineering

2a. REPORT SECURITY CLASSIFICATION

AD/A-005645

2b. GROUP

3. REPORT TITLE

Acoustic Surface Wave Devices for Visible and Infrared Imaging

4. DESCRIPTIVE NOTES (Type of report and inclusive dates)

Semi-Annual Technical Report; 6/1/74 - 11/30/74

5. AUTHOR(S) (Last name, first name, initial)

Gunshor, Robert L.

6. REPORT DATE	7a. TOTAL NO. OF PAGES	7b. NO. OF REFS
January 1, 1975	20	8

8a. CONTRACT OR GRANT NO.	9a. ORIGINATOR'S REPORT NUMBER(S)
DAHC15-73-G12	
b. PROJECT NO. ARPA Order No. 2340 Amendment No. 1	
c.	9b. OTHER REPORT NO(S) (Any other numbers that may be assigned this report)
d.	

10. AVAILABILITY/LIMITATION NOTICES

Distribution of this document is unlimited.

11. SUPPLEMENTARY NOTES	12. SPONSORING MILITARY ACTIVITY
	Defense Advanced Research Projects Agency 1400 Wilson Blvd. Arlington, Virginia 22209

13. ABSTRACT

The objective of this research is the conception, development, and critical evaluation of a new class of devices employing the nonlinear interaction of acoustic surface waves (ASW) and photo-excited charge carriers to achieve rapid-scan optial imaging. The device operating principles are to be demonstrated initially through the use of silicon; however, a major objective is to obtain imaging with infrared radiation using narrow bandgap semiconductors. The experimental effort involves both separate medium and monolithic device configurations.

DD FORM 1 JAN 64 1473

UNCLASSIFIED

Security Classification

14 KEY WORDS	LINK A		LINK B		LINK C	
	ROLE	WT	ROLE	WT	ROLE	WT
Optical Imaging with Acoustic Surface Waves						

INSTRUCTIONS

1. ORIGINATING ACTIVITY: Enter the name and address of the contractor, subcontractor, grantee, Department of Defense activity or other organization *(corporate author)* issuing the report.

2a. REPORT SECURITY CLASSIFICATION: Enter the overall security classification of the report. Indicate whether "Restricted Data" is included. Marking is to be in accordance with appropriate security regulations.

2b. GROUP: Automatic downgrading is specified in DoD Directive 5200.10 and Armed Forces Industrial Manual. Enter the group number. Also, when applicable, show that optional markings have been used for Group 3 and Group 4 as authorized.

3. REPORT TITLE: Enter the complete report title in all capital letters. Titles in all cases should be unclassified. If a meaningful title cannot be selected without classification, show title classification in all capitals in parenthesis immediately following the title.

4. DESCRIPTIVE NOTES: If appropriate, enter the type of report, e.g., interim, progress, summary, annual, or final. Give the inclusive dates when a specific reporting period is covered.

5. AUTHOR(S): Enter the name(s) of author(s) as shown on or in the report. Enter last name, first name, middle initial. If military, show rank and branch of service. The name of the principal author is an absolute minimum requirement.

6. REPORT DATE: Enter the date of the report as day, month, year, or month, year. If more than one date appears on the report, use date of publication.

7a. TOTAL NUMBER OF PAGES: The total page count should follow normal pagination procedures, i.e., enter the number of pages containing information.

7b. NUMBER OF REFERENCES: Enter the total number of references cited in the report.

8a. CONTRACT OR GRANT NUMBER: If appropriate, enter the applicable number of the contract or grant under which the report was written.

8b, 8c, & 8d. PROJECT NUMBER: Enter the appropriate military department identification, such as project number, subproject number, system numbers, task number, etc.

9a. ORIGINATOR'S REPORT NUMBER(S): Enter the official report number by which the document will be identified and controlled by the originating activity. This number must be unique to this report.

9b. OTHER REPORT NUMBER(S): If the report has been assigned any other report numbers *(either by the originator or by the sponsor)*, also enter this number(s).

10. AVAILABILITY/LIMITATION NOTICES: Enter any limitations on further dissemination of the report, other than those imposed by security classification, using standard statements such as:

(1) "Qualified requesters may obtain copies of this report from DDC."

(2) "Foreign announcement and dissemination of this report by DDC is not authorized."

(3) "U. S. Government agencies may obtain copies of this report directly from DDC. Other qualified DDC users shall request through _____."

(4) "U. S. military agencies may obtain copies of this report directly from DDC. Other qualified users shall request through _____."

(5) "All distribution of this report is controlled. Qualified DDC users shall request through _____."

If the report has been furnished to the Office of Technical Services, Department of Commerce, for sale to the public, indicate this fact and enter the price, if known.

11. SUPPLEMENTARY NOTES: Use for additional explanatory notes.

12. SPONSORING MILITARY ACTIVITY: Enter the name of the departmental project office or laboratory sponsoring *(paying for)* the research and development. Include address.

13. ABSTRACT: Enter an abstract giving a brief and factual summary of the document indicative of the report, even though it may also appear elsewhere in the body of the technical report. If additional space is required, a continuation sheet shall be attached.

It is highly desirable that the abstract of classified reports be unclassified. Each paragraph of the abstract shall end with an indication of the military security classification of the information in the paragraph, represented as *(TS), (S), (C), or (U)*.

There is no limitation on the length of the abstract. However, the suggested length is from 150 to 225 words.

14. KEY WORDS: Key words are technically meaningful terms or short phrases that characterize a report and may be used as index entries for cataloging the report. Key words must be selected so that no security classification is required. Identifiers, such as equipment model designation, trade name, military project code name, geographic location, may be used as key words but will be followed by an indication of technical context. The assignment of links, rules, and weights is optional.

GPO 886-551

Summary

The objective of this research is the conception, development and critical evaluation of a new class of devices employing the nonlinear interaction of acoustic surface waves (ASW) and photo-excited charge carriers to achieve rapid-scan optical imaging. The device operating principles are to be demonstrated initially through the use of silicon; however, a major objective is to obtain imaging with infrared radiation using narrow bandgap semiconductors. The experimental effort involves both separate medium and monolithic device configurations.

The research is designed to emphasize the demonstration of two newly envisioned device concepts for ASW imaging using silicon. The devices initially are fabricated using silicon in order to benefit from the well developed understanding and controllability of silicon surface properties. One of these devices, a transverse parametric imaging device, in addition to increased dynamic range, is expected to read an image in a time that is at least one-tenth of other proposed ASW devices.

The second device, for which operation is based on second harmonic generation, has been successfully operated as an imager, with significantly better performance than previously reported devices depending on attenuation to form the image. The actual advantage achieved by the second harmonic generation device was about 10 db, although as much as a 30 db increase in dynamic range is possible.

A study of a ZnO-silicon monolithic configuration for acoustic surface wave imaging was begun in collaboration with the Naval Research Laboratory. The result of this effort is an optical imaging device not requiring an air gap.

On the analytical side, a new large-signal convolution theory has been developed which will account for previously unexplained results from ASW convolution experiments.

The research program will continue to explore the above mentioned device concepts, and additionally provide critical evaluations of these and other ASW devices proposed for optical imaging.

Contents

I. Second Harmonic Generation for Optical Imaging*

(R. L. Gunshor, P. S. Schenker, C. W. Lee)

Recently reported ASW optical image devices transform spatial variations in light intensity to a corresponding set of amplitude variations in time on an electrical signal. This is accomplished by coupling rf surface waves propagating on a piezoelectric substrate to an adjacent semiconductor medium; the light-perturbed surface charge density is spatially variant along the path of ASW propagation. Reported devices differ in the wave-particle interaction phenomenon employed to obtain the image. Moll, et al.,[1] describes a device which achieves image conversion via light induced signal attenuation. Takada, et al.,[2] describes a device based on image induced variations in the longitudinal acoustoelectric voltage, and Luukkala and Meriläinen[3] report a device that senses the coupled impedance mismatches resulting from light induced spatial discontinuities in surface charge density. This report concerns ASW conversion of optical images with light enhancement of second harmonic generation as the wave-particle interaction mechanism. Similar in configuration to the device reported by Moll, et al., the device described here employs two contrapropagating surface waves to form the converted image signal. One pulse serves as the power source for harmonic generation while another higher power pulse imparts image information to the harmonic by local decoupling of the semiconductor-ASW interaction. The second harmonic and its copropagating fundamental source will subsequently be referred to as reading signals; the higher power contrapropagating signal is termed a decoupling pulse.

*(This work is reported in Applied Physics Letters, December 15, 1974)

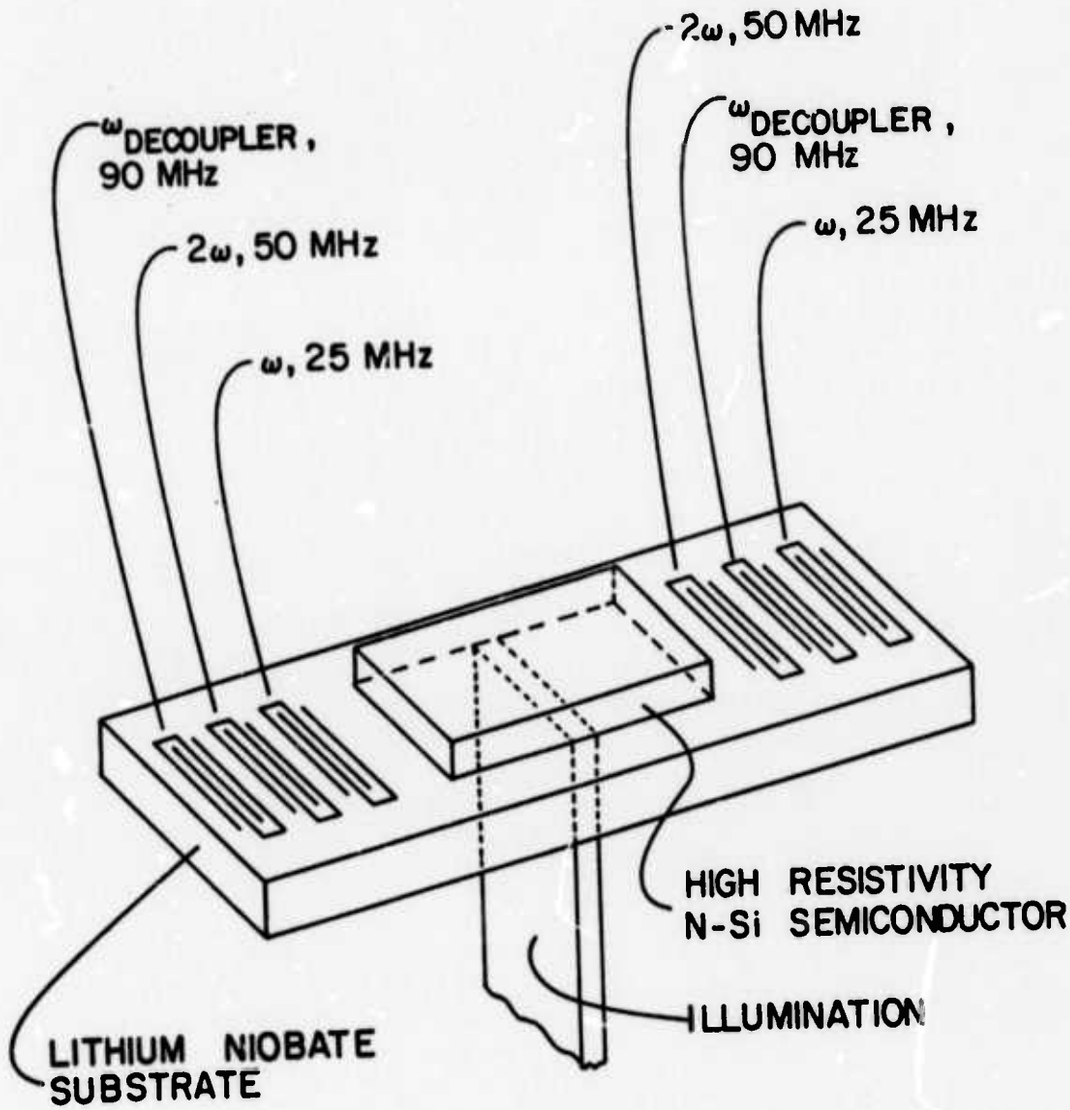

THE EXPERIMENTAL DEVICE

FIG. 1 Experimental Device: Fundamental and Second Harmonic Frequencies are 25 and 50 MHz Respectively and Decoupler Input is at 90 MHz

The use of harmonic generation for optical imaging makes available the 40 db dynamic range associated with second harmonic generation of ASW in the presence of a semiconductor.[4] This effect portends a large harmonic signal amplitude variation for surface carrier density variations introduced by a given range of light intensity. In addition, unlike a device which is based on light-induced attenuation of the fundamental, output in the dark can approach zero.

Description of Experiment

Figure 1 shows the device configuration. Experiments were performed using a 5.0 cm long, 1.2 cm wide, 1 mm thick YZ-cut lithium niobate substrate with aluminum interdigital transducers fabricated using conventional photolithographic techniques. A 0.25 mm thick, 1.25 cm long nominal 1000 Ω-cm n-silicon sample is pressed into intimate contact with the substrate surface, achieving coupling between the rf piezoelectric fields associated with the acoustic surface waves and charge carriers in the semiconductor. The fundamental frequency wave is launched by a five finger pair interdigital transducer designed for 25 MHz; harmonic output is taken from a five finger pair interdigital transducer at 50 MHz. The decoupling pulse is introduced at 90 MHz via a ten finger pair interdigital transducer. Transducers are fabricated in pairs (Fig. 1) to allow conventional delay line measurements; the beam width of all transducers is 2 mm. The harmonic output is bandpass filtered at 50 MHz and displayed on a 250 MHz cathode ray oscilloscope. Output at the 25 MHz fundamental frequency may likewise be displayed on the oscilloscope for purposes of comparing images formed by harmonic generation and those produced by attenuation phenomenon.

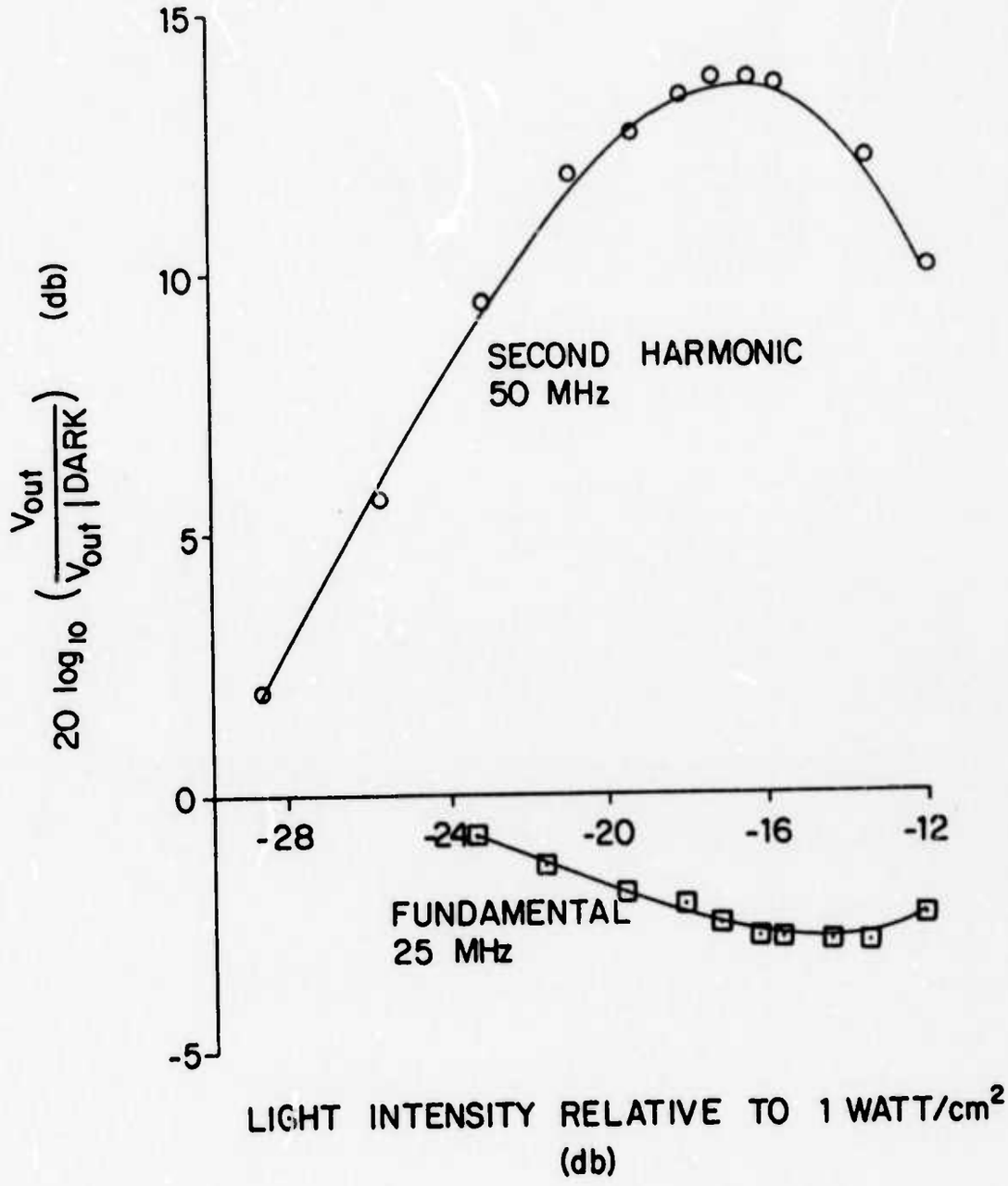

FIG. 3. Plot of 20 $\log_{10}$(output voltage/output voltage in the dark) vs intensity of illumination of a 2-mm wide strip of light for fundamental and second harmonic output.

The experiment is performed in the following manner. The fundamental and contrapropagating decoupling pulse are synchronized in time at t_o such that the leading edge of the reading pulse and trailing edge of the decoupling pulse coincide at the output edge of the semiconductor. Encoding of the image information onto the reading pulse is complete when the decoupling pulses arrives at the input end of the semiconductor. The decoupler pulse leading edge is now coincident with the reading pulse trailing edge; this occurs at approximately $t_o + \frac{\ell}{v_s}$ where v_s is the surface wave velocity and ℓ is the semiconductor length. Therefore the reading pulse must have a length 2ℓ. Spatial variations in optical intensity along the beam path are thereby expanded in time by a factor of two due to the contra-flow process.

In the absence of a decoupling pulse all portions of the reading signal will experience an identical interaction with the photo-excited charge carriers. Introduction of the decoupling pulse results in significantly reduced interaction[5] between charge carriers and the reading pulse at the locale of the decoupling pulse. Thus, the fundamental experiences a localized relaxation in attenuation and the harmonic a localized loss of charge carrier enhancement correlated to the charge density at the decoupled locale. This ultimately results in a dip in harmonic output whose time of occurence and duration corresponds to the position and length of an optical disturbance of the semiconductor surface charge density. Simultaneously, the fundamental output displays an image that is the "negative" of the second harmonic image. The choice of duration of the decoupling pulse is a compromise between image size and resolution; a short pulse is beneficial to resolution but leading to reduced signal-to-noise ratio in the output.

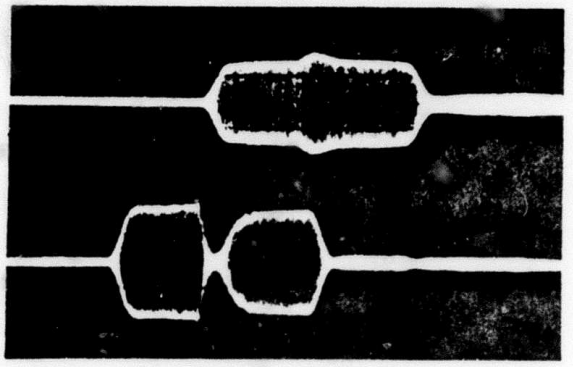

a

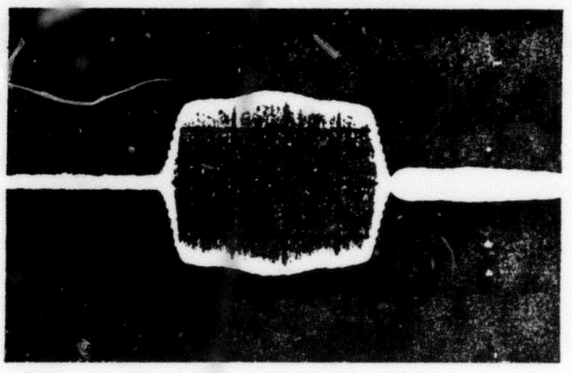

b

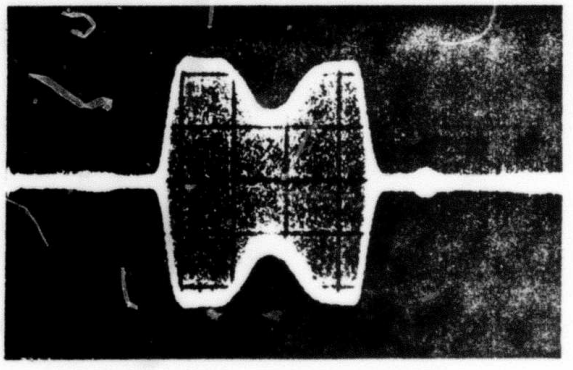

c

FIG. 2 (a) Effect of 0.3-μsec copropagating decoupling pulse on fundamental and second harmonic. (b) Fundamental image (25 MHz). (c) Second harmonic image (50 MHz). Horizontal scale for all traces is 1 μsec/div.

Experimental Results

Figure 2a demonstrated the ability of the decoupling pulse to remove charge carriers from interaction with the reading pulse. This display is obtained by copropagating reading and decoupling pulses under a semiconductor illuminated with a 2 mm wide strip of white light (Fig. 1). The previously described reduction in harmonic enhancement and relaxation of attenuation is observed where the decoupling and reading pulses are coincident.

Figures 2b,c respectively, show the fundamental and harmonic outputs when the experimental configuration is prepared for imaging by contrapropagating the decoupling pulse with the reading pulse in proper synchronization. The experimental parameters are the same as for Fig. 2a. The results of Figs. 2b,c are obtained by optimizing the experimental parameters for best image display in each case.

Figure 3 shows how the fundamental and second harmonic vary as a function of light intensity in the absence of a decoupling pulse, again a 2 mm strip of incident illumination is used. In both cases one observes a saturation intensity; this light level is a function of semiconductor dark resistivity, surface preparation, air gap, and choice of operating frequency. For a given variation in incident light intensity it is apparent that a greater variation in amplitude occurs for the harmonic than for the fundamental.

Figure 4 shows the image of two illuminated strips respectively 0.3 mm and 0.6 mm wide separated by 1.0 mm. The display is obtained using the second harmonic output scheme. The dimensions of strip widths and spacing correspond to two, four, and seven wavelengths at the fundamental frequency.

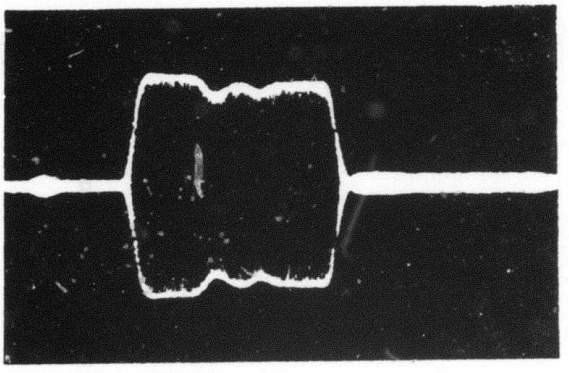

FIG. 4 Second harmonic image of two slits.

The level of illumination used for Figs. 2 and 3 was 10 db above 1 mW/cm^2; the level of illumination producing unity signal-to-noise ratio in the second harmonic output is found to be about 6 db below 1 mW/cm^2 at 6328 Å.

II. Optical Imaging with a ZnO-Si Monolithic Device

(R. L. Gunshor, R. F. Pierret, J. K. Elliott, K. L. Davis*)

The device consists of a 1.2 micron rf-sputtered ZnO layer on 300 Ω-cm (111) n-silicon. A pair of interdigital transducers launch pulse modulated input signals at 179 MHz, and a convolution output is obtained from a thin (transparent) aluminum gate electrode on top of the ZnO. The input pulse lengths are 3.0 μsec and 100 nsec; the width of the narrower pulse determines the resolution of the imager.

Measurements have been made of image output for various light intensities and dc gate voltages. Resolution limits have been observed using projected images of alternating light and dark strips.

A complete discussion of this work will appear in the final report.

*Dr. Davis is at the Naval Research Laboratory, Washington D. C.

III. Large-Signal Acoustic Surface Wave (ASW) Convolver Response Theory

(R. F. Pierret and R. L. Gunshor)

Work is in progress to develop a simple large-signal response theory for the ASW convolver, one of the structures under consideration for projected ASW imaging applications. In such applications, and in design considerations, a simple response theory is clearly desirable. Incorporating metal-insulator-semiconductor modeling and formalism, we have derived the large signal circuit representation for the convolver shown in Fig. 5. Using this circuit representation, we have already established simple theoretical expressions for the convolver output; we are in the process of making quantitative comparisons between the predicted convolver output and the output derived from experimental ZnO-SiO_2-Si structures. Preliminary comparisons between experiment and theory are excellent. Detailed comparisons with experiment, relative evaluation of competing convolver variations, design optimization and extension of the theory to the transverse acoustoelectric effect are all part of the ongoing program.

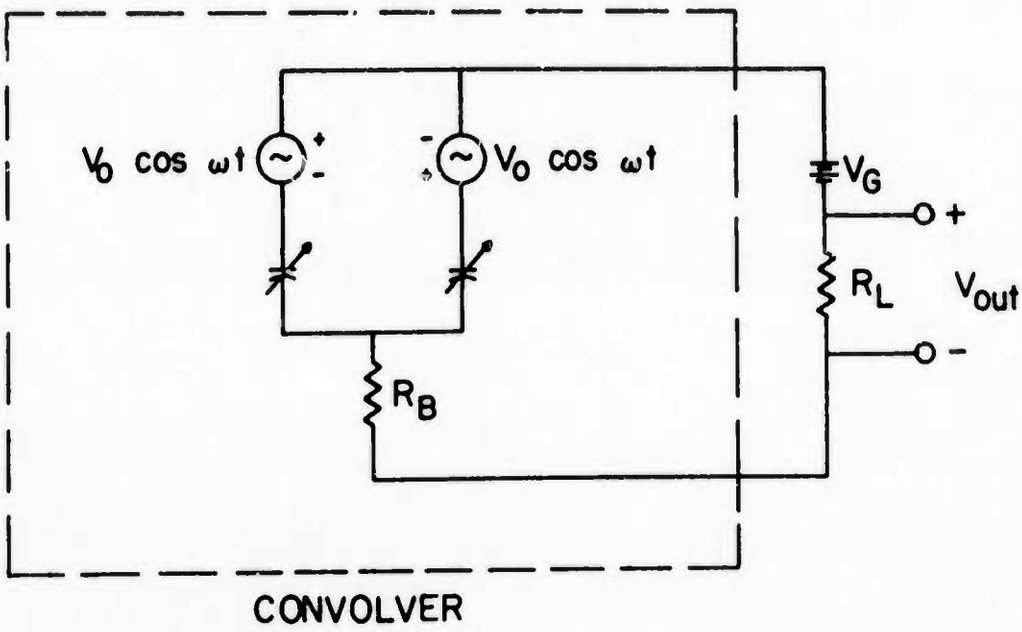

FIG. 5

IV. Acoustic Surface Wave Measurement of Majority Carrier Mobility

(R. F. Pierret and R. L. Gunshor)

In a recent publication Bers, et al.[6] utilized acoustic surface wave (ASW) techniques to ascertain the effective mobility of near surface carriers in a semiconductor accumulation layer. Their experimental configuration consists of a high resistivity n-silicon sample placed on top of a lithium niobate substrate. The ASW is launched on the lithium niobate, and propagates under the silicon. The piezoelectric fields associated with the ASW tend to produce a drift of electrons along the direction of propagation. The resulting direct current, called an acoustoelectric current, is measured and used to compute the value of the surface mobility. The cited paper was significant in that it illustrated the potential of ASW techniques in probing semiconductor surface properties. Unfortunately, Bers, et al. compared their experimental results against earlier non-ASW experimental results and a theoretical formulation all specifically concerned with minority carriers in surface inversion layers.

We note that the appropriate theory for majority carriers in accumulations layers was first formulated by Greene, et al.[7] and was later presented in a more convenient form by Goldstein, et al.[8] For the Bers, et al. structures and the normalized surface potential (U_S) range probed, the thecretical effective mobility to bulk mobility ratio (μ_{eff}/μ_B) is accurately approximated by

$$\frac{\mu_{eff}}{\mu_B} = 1 - \frac{r}{\sqrt{2}} e^{-U_S/2} \int_{U_S-7}^{U_S} e^{x}[1 - e^{-f(x)/r}]dx \qquad (1)$$

where

$$f(x) = e^{-x/2} \operatorname{erf}\sqrt{(U_S - x)/2} \tag{2}$$

and $r = 0.001$. The preceding majority carrier theory and the Bers, et al. experimental results are compared in Fig. 6. Very good agreement between the corrected theoretical predictions and the ASW measured mobilities is clearly evident.

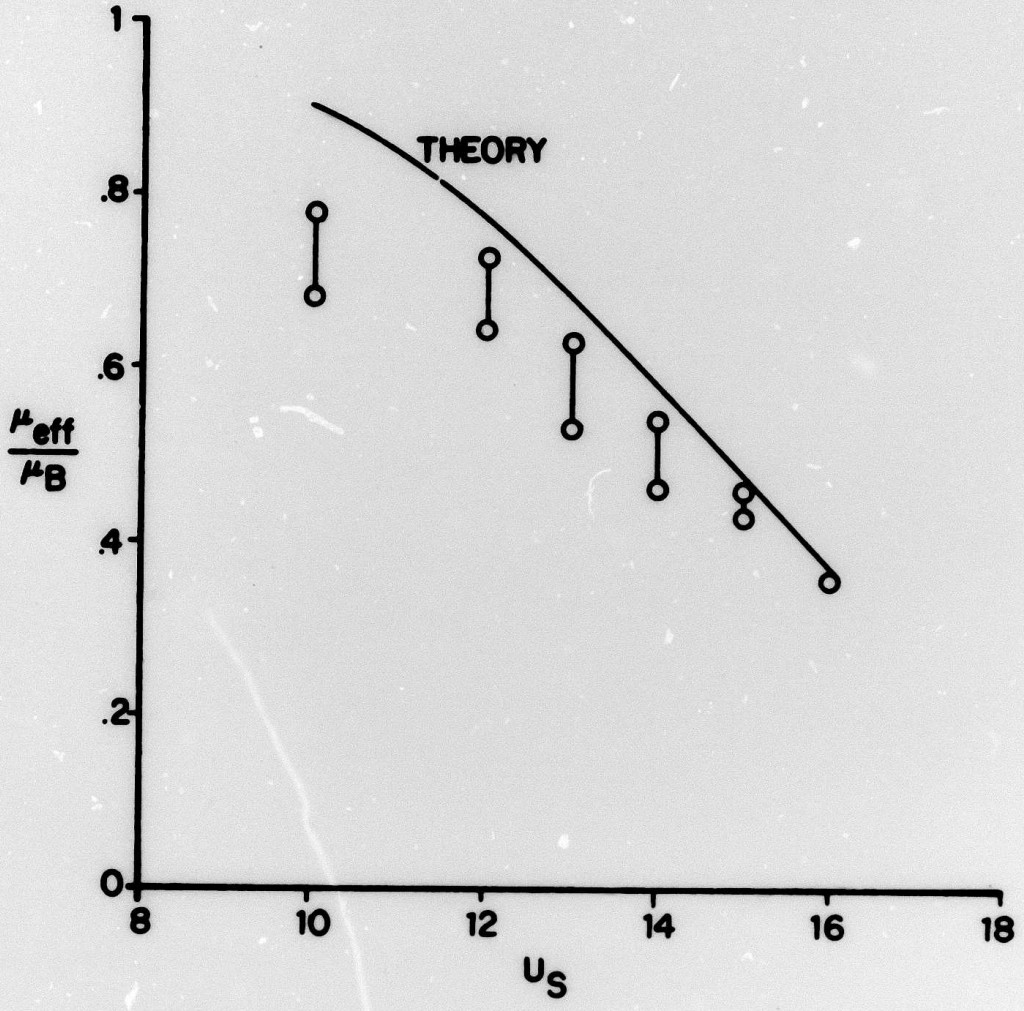

FIG. 6 Comparison of accumulation layer effective mobility theory and ASW derived experimental results. (O—O range of Bers et. al data derived from three similar test structures.)

References

1. N. J. Moll, O. W. Otto, and C. F. Quate, Journal de Physique 33, Supplement to No. 11-12, 231 (1972).
2. S. Takada, H. Hayakawa, and N. Mikoshiba, Appl. Phys. Letters 23, 415 (1973).
3. M. Luukkala and P. Meriläinen, Electron. Letters 10, 80 (1974).
4. C. W. Lee and R. L. Gunshor, Appl. Phys. Letters 20, 288 (1972).
5. C. W. Lee and R. L. Gunshor, J. Appl. Phys. 44, 4807 (1973).
6. A. Bers, J. H. Cafarella and B. F. Burke, "Surface mobility measurements using accustic surface waves," Appl. Phys. Letts., 22, 399 (April 15, 1973).
7. R. F. Greene, D. R. Frankl and J. Zemel, "Surface transport in semiconductors," Phys. Rev., 118, 967 (May, 1960).
8. Y. Goldstein, N. B. Grover, A. Many, and R. F. Greene, "Improved representation of calculated surface mobilities in semiconductors. II. Majority carriers," J.A.P., 32, 2540 (December, 1961).